

F. SIZOV

V.E. Lashkaryov Institute of Semiconductor Physics
(41, Nauky Av., Kyiv 03680, Ukraine; e-mail: sizov@isp.kiev.ua)

UNCOOLED WIDE-RANGE SPECTRAL OPTOELECTRONIC DEVICES ON THE BASE OF HgCdTe SEMICONDUCTOR

PACS 85.60.Gz, 85.30.De

Issues associated with the development and the exploitation of infrared (IR) and sub-terahertz (THz) radiation detectors based on HgCdTe semiconductor are discussed. It is shown that this mercury cadmium telluride (MCT) semiconductor can be applied to the development of bi-colour detectors operating in the IR and sub-THz spectral ranges.

Keywords: MCT, IR and sub-THz detectors.

1. Introduction

Light and other electromagnetic waves are the main sources for obtaining the information about the environment by means of different kinds of detectors, which play an important role in different areas of the human activity (e.g., in the imaging, medicine, biology, astronomy, materials testing, security, etc.). For these tasks, one uses the interaction of electromagnetic waves with matter not only in the region visible by human eyes ($\lambda \approx 0.4\text{--}0.75 \mu\text{m}$), but also in other “invisible” various spectral bands: radio frequencies, microwaves, THz, IR, ultraviolet, as well as X-rays and higher energy radiation. All the phenomena rely on the physical effects related to the interaction of electromagnetic waves with bodies and substances. The key role in obtaining the information about such interaction is played by detectors, which should operate in different spectral ranges. It would be desirable to have detectors based on a small number of available material technologies or even, in the ideal case, on one material, thus restricting the technologies of their manufacture. However, the realization of detectors based on few materials or even one material is a challenge because of the detector sensitivities in different spectral ranges are based on different physical phenomena, and, as a rule, these different phenomena cannot be implemented with one material.

One of such materials can be MCT semiconductor ($\text{Hg}_{1-x}\text{Cd}_x\text{Te}$), the band-gap of which can be varied by altering the composition from $x = 1$ (CdTe band gap $E_g \approx 1.6 \text{ eV}$) to $x \approx 0.165$ (band gap $E_g \approx 0 \text{ eV}$).

MCT is the material of choice for many IR focal plane array (FPA) applications. The characteristics of this semiconductor, especially for the composition $x \approx 0.2\text{--}0.3$, were widely discussed, since they as detectors are suitable for 3–5 and 8–12 μm atmosphere transparency regions, though they should be cooled, as a rule, to $T \approx 80\text{--}150 \text{ K}$ (see, e.g., [1]). Low leakage currents and high carrier mobility in MCT detectors result in the possible upper limit performance.

As one of the examples of applications of MCT-based materials in optoelectronic devices today, we mention one of the most effective CdTe solar energy converters, which are produced commercially [2]. CdTe (and also CdZnTe) is one of the most important materials for the manufacture of un-cooled X/ γ -ionizing radiation detectors of the spectrometric type, especially for the energy range $E > 30\text{--}50 \text{ eV}$ [3]. This MCT semiconductor can be used for the detector production not only for the atmospheric transparency regions from 3 to 5 and from 8 to 14 μm , but for the short-wave IR wavelength region ($\sim 0.8\text{--}3.0 \mu\text{m}$) as well (see, e.g., [1]).

MCT is the best solution for single- and multiband systems covering a wide range of wavelengths, because it is possible to tune the wavelength by selecting the appropriate composition. Moreover, it is possible to design and to grow structures, where the composition is tuned in such a manner that two or more wavelengths are operational within a single device.

Important would be an expansion of the MCT detectors sensitivity to the THz/sub-THz electromagnetic radiation region topical today because of the nondestructive testing possibility (due to low-energy non-ionizing radiation), security applications, com-

munications, imaging, etc. (see, e.g., [4]). But tuning the chemical composition to x giving $E_g \Rightarrow 0$ (at $\lambda \approx 300 \mu\text{m}$, $\nu = 1 \text{ THz}$, $h\nu \approx 4 \text{ meV}$, as compared to the thermal energy at 26-meV room temperature), which is needed for cost-effective THz detectors, leads to a very high thermo-generation rate of carriers [5] preventing the efficient THz/sub-THz detector operation based on interband transitions.

As for THz/sub-THz detector techniques, except the tendency to implement the detector arrays allowing the better detection performance, these techniques are desirable to be completed with other available technologies, e.g., those allowing simultaneously the operation in other spectral regions to make such systems more informative. To use uncooled MCT THz detectors was first offered in [6], while analyzing the properties of a free electron gas heated by THz radiation. It was shown that three following effects are responsible for the sensitivity of sub-THz/THz MCT detectors with intrinsic conductivity [7]: (i) Demer effect (photo-diffusion effect) contribution, (ii) thermo-electromotive contribution, and (iii) contribution that is associated with free carrier concentration changes.

It can be noted that the summation of these three effects, when changing their contribution with temperature or free carrier concentration, can be the reason for the negative “photoconductivity” in the sub-THz/THz spectral range, which was observed experimentally. Such THz/sub-THz uncooled detectors were realized in [7, 8].

The purpose of this investigation is to show the possibility to realize the uncooled detector operation both in the infrared (IR) and sub-THz spectral regions within the same chip. Really, it is feasible to apply one chip detector and in the short IR wavelength region ($\lambda \sim 0.8 \mu\text{m}$), if the substrate CdTe for growing MCT layers is used.

To apply MCT layers both in the IR and sub-THz regions, the detectors with the active area $\sim 50 \times 25 \mu\text{m}$ in size were prepared. The rectangular form of a sensitive element was chosen for increasing the detector resistance of the active area to approach the antenna impedance Z which is near 100–200 Ω for a bow-tie antenna used.

The longer dimension of the active part area of the detector is near the Airy disk diameter A_{dif} for the spectral range of 8–14 μm . Within the Airy disk area, about 84% of the light energy are concentrated

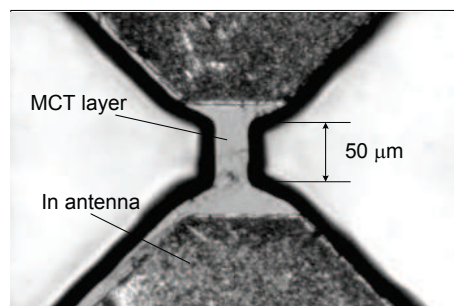


Fig. 1. MCT sensitive element with bow-tie antenna

($A_{\text{dif}} = 2.44 \times \lambda \times (f/D)$, where f is the lens focus length, and D is the lens diameter). At this area, the IR radiation is absorbed directly. For the sub-THz/THz radiation energy transfer into this active area, the antennas with dimensions about the wavelength length are used. For the IR detector, both *In* antenna blades serve as electrical contacts (see Fig. 1).

Most of IR and THz/sub-THz technologies are connected with the imaging. These two technologies still differ in numerous aspects. The infrared imaging is an efficient passive technology, whereas the THz one is, as a rule, an active one requiring some sources for the illumination of examined objects. Moreover, these detectors are typically also different in operational principles. For example, one of these differences lies in the sizes of a detector. The infrared detectors (their sensitive elements) are about or a little bit smaller than the wavelengths (connected with Airy disk diameter A_{dif}), whereas the THz/sub-THz ones, though having similar proportions, are compared to the wavelength, but only with regard for the antenna dimensions about the wavelength length. The sensitive elements of THz/sub-THz detectors typically are much smaller than the radiation wavelength and smaller than the detector area for the IR region. This results in different constraints when designing the imaging systems [9]. Another difference lies in different physics of introduction the radiation into a sensitive element. In the IR detectors, it is a direct absorption of radiation by a sensitive element, while the radiation power in THz/sub-THz detectors is typically introduced in a sensitive element by the antenna.

In MCT IR photoconductors, the changes in the conductivity arising under the IR illumination result in the photoconductor response due to valence-to-conduction band transitions as in other typical in-

trinsic photoconductors. In MCT sub-THz/THz hot-electron-bolometers (HEB), the response is due to heating the electron gas with the power introduced via the antenna and the motion of free carriers in a sensitive element [7]. This motion is governed by three different effects, which can lead, under THz radiation, both to increasing or decreasing the detector conductivity.

At low radiation powers, the MCT IR and sub-THz/THz detectors are square-law ones, in which the response is proportional to the incoming radiation power, and both IR and THz/sub-THz detectors can be assembled into arrays.

2. IR/sub-THz MCT Detectors

Terahertz (THz) technologies (radiation frequencies loosely defined from the frequencies $\nu \sim 0.1$ THz to 10 THz [4, 10] ($\lambda \sim 3$ mm–30 μ m)) are emerging ones now, which promises a wide choice for potential applications to the vision systems, high-speed wireless communications, spectroscopy, medicine, security, etc. [11]. They can give images with a relatively high resolution. At the same time in the case of active imaging, THz radiation is not ionizing, as its photons are not energetic enough to knock electrons off atoms and molecules, e.g., in a human body. Along with sources, the important components of these technologies are detectors. In many applications, the uncooled detectors capable for the integration into arrays are desirable in order to obtain the real-time imaging.

Unfortunately, the atmosphere transparency and the spectral radiance are poor in the THz spectral region. This leads to the situation where the passive imaging in this spectral range even with highly sensitive deeply cooled detectors is restricted by several tens of meters [11]. At the same time, there are possible short-range (within the distance pointed out) wireless high information capacity communications without using the special restricting methods of information loose to unwanted users. In the low-frequency region ($\nu \leq 0.5$ THz, the wavelength in vacuum $\lambda = c/\nu \geq 600$ μ m, where c is the speed of light) of THz spectra, the radiation can penetrate most nonmetallic and nonpolar substances. Therefore, the imaging applications are a substantial part of the technological development in this direction.

For the cost-effective and space-limited THz vision, important is the use of uncooled detectors, since

the deeply cooled ones are bulky and expensive in production and operation. To estimate the sensitivity limit, which should be achieved for the uncooled detectors to operate in a passive regime, one can use such parameter as the so-called noise equivalent power (NEP), which characterizes the detector sensitivity as a minimal signal registered at the noise level of the detector itself or noise from the background radiation.

For THz/sub-THz region of ~ 0.4 –0.1 THz and typical spectral resolution $\Delta\lambda/\lambda \sim 0.3$ appropriate for the imaging for a diffraction-limited direct-detection detector with dimensions close to the Airy disk diameter, one can estimate the required detector pixel NEP for an optical system with the aperture input diameter $D \approx 0.5$ m, the distance between the aperture and the object $R \approx 5$ m, and for the focal length $f \approx D$ (f -number $F/\# \approx 1$) (if the detectivity $D^*(\lambda) \sim \text{const}$ for thermal detectors), by using an expression [12]

$$\text{NEP} \approx \frac{\text{NETD } A_d \sqrt{\eta} \int_{\lambda_{co}}^{\lambda_u} \frac{\partial P(\lambda, T)}{\partial T} d\lambda}{4}. \quad (1)$$

Here, η is the detector quantum (coupling) efficiency, and $\frac{\partial P(\lambda, T)}{\partial T}$ is the derivative of Planck's curve. The coefficients τ_{op} , τ_{atm} , and τ_f which are the transmission coefficients of optics, the atmosphere, and a filter, respectively, were taken to be 1. Therefore, these coefficients are omitted in Eq. (1). Then, for the spectral region $\lambda_1 \approx 0.85$ mm, the spectral band width $\Delta\lambda/\lambda \approx 0.3$ ($\lambda_{co} \approx 0.7$ mm, $\lambda_u \approx 1.0$ mm), $\eta = 1$, and the practically sufficient temperature resolution $\Delta T \approx 0.1$ K, the value of $\text{NEP}_1(\Delta T = 0.1\text{K}) \approx 1.3 \times 10^{-12}$ W. For the longer wavelength region $\lambda_1 \approx 3.0$ mm and for the same spectral band width $\Delta\lambda/\lambda \approx 0.3$ ($\lambda_{co} \approx 2.5$ mm, $\lambda_u \approx 3.5$ mm), $\text{NEP}_2(\Delta T = 0.1\text{K}) \approx 4 \times 10^{-13}$ W. In both cases, it is accepted that the background temperature T is the black-body temperature $T = T_{bb} = 310$ K.

For the frame rate $f_r \approx 10$ Hz, the integration time $t_{int} \approx 10^{-1}$ s for a single detector, and the noise equivalent bandwidth $\Delta f_e = (2 \times t_{int})^{-1} \approx 5$ Hz. Then, for the detector pixel performance, we estimated $\text{NEP}_1(\Delta T = 0.1 \text{ K}) \approx 6 \times 10^{-13}$ W/Hz^{1/2} and $\text{NEP}_2(\Delta T = 0.1 \text{ K}) \approx 2 \times 10^{-13}$ W/Hz^{1/2}, respectively. If the coupling efficiency $\eta \sim 0.1$ –0.3 (for the detector with a wide frequency band antenna, as

a rule, this is a case for THz/sub-THz detectors) then these values should be multiplied by $\eta^{1/2}$.

From the detector parameters with NEP $\sim 10^{-12}$ W/Hz^{1/2}, the arrays with $M \geq 10$ detectors allow one to realize almost the real-time passive direct detection imaging systems with the frame rate of $f_r \sim 10$ Hz and the requirements of $\Delta T \sim 0.5$ K, by using, e.g., uncooled Schottky barrier diode detectors (NEP $\sim 10^{-12}$ W/Hz^{1/2} [13, 14]). Other types of uncooled detectors have NEP $> 10^{-10}$ – 10^{-11} W/Hz^{1/2} (see, e.g., [5] and references therein) and can be used only in active imaging systems or, perhaps, in low resolution systems with a larger number of detectors in an array, which allows one to decrease the requirements to the detectors.

As a rule, the thickness of active layers for ordinary MCT photoconductive detectors is ≥ 10 μm . To improve the impedance matching of a THz MCT bolometer active layer with an antenna, it is desirable to make its active layer thinner. Estimations for IR detectors have shown that the base of the IR response even at $T = 300$ K is that the band-to-band optical absorption is strong in a direct-gap MCT semiconductor with chemical composition $x \approx 0.21$ ($E_g(300\text{ K}) \approx 0.17$ eV $\Rightarrow \lambda_{\text{co}} \approx 7.4$ μm). At $\lambda \approx 5$ μm and $T = 300$ K, the absorption coefficient α in such layers is $\alpha \approx 5 \times 10^{-3}$ cm⁻³. Thus, in the active layers with the thickness $d \approx 5$ μm , the approximation of strong absorption ($\alpha d > 1$) is still valid. Since the diffusion length is much larger than the thickness of the active layer, there will exist approximately the same generation rate $g(d)$ under illumination at any absorption depth:

$$g(d) = d^{-1} \eta_i (1 - R) N_{\text{ph}}, \quad (2)$$

where η_i is the inner quantum efficiency (for MCT, $\eta_i \approx 1$), R is the reflection coefficient ($R \approx 0.34$), and N_{ph} is the number of photons falling down on the active area of a photoconductor. From Eq. (2), it follows that the responsivity will be inversely proportional to the depth of the active layer of a photoconductor that was proved experimentally for photoconductors on the base of similar layers grown by molecular beam epitaxy (MBE) [15]. Our research showed that the highest responsivity within the different layers was observed in a detector with the active layer thickness $d = 4$ μm . Following this tendency, we took the layers with thicknesses d that are less than the

typical thickness $d \sim 10$ μm for these photoconductors. To increase the impedance of MCT active layers, the p -type layers with the life time $\tau \sim 5 \times 10^{-8}$ s were chosen to manufacture the detectors.

We considered the possibility to use the well-known MCT layers as detectors in the sub-THz radiation frequency range $\nu \sim 70$ – 150 GHz and also as photoconductors in the IR spectral region from 3 to 12 μm . Such bi-color THz/sub-THz hot electron bolometer and IR photoconductor consist of metal bow-tie antennas deposited directly onto MCT epitaxial layers with GaAs substrates with the thickness $d \sim 400$ μm and the high permittivity $\varepsilon \approx 13$ (see Fig. 1). It is not an effective design of sub-THz detectors as the thickness of a high-permittivity substrate does not allow one to obtain an optimized NEP in the sub-THz spectral region. But such design was applied to demonstrate the responsivity of MCT detectors both in the sub-THz and IR regions. The input of radiation into the detecting elements from antennas on low-permittivity substrates is much more effective, as compared to antennas that are formed directly on substrates with a high dielectric permittivity at comparable thicknesses. The hybridizing technology of small-area detectors with antennas on substrates with a low dielectric permittivity [8] at room temperature allowed one to reach NEP $\approx 2.6 \times 10^{-10}$ W/Hz^{1/2} in the $\nu \approx 128$ – 144 GHz radiation frequency range.

Here, the THz/sub-THz response of MCT detectors is observed in p -type layers with the hole concentration $p_{78\text{ K}} \approx 5.6 \times 10^{15}$ cm⁻³, $p_{78\text{ K}} \approx 5.7 \times 10^{15}$ cm⁻³ at $T = 78$ K for the chemical compositions $x \approx 0.224$, and $x \approx 0.214$, and the thicknesses of MCT layers to be 7.8 μm and 6.3 μm , respectively. These layers at $T = 300$ K have intrinsic conductivity with the intrinsic concentration $n_i \approx 2.0 \times 10^{16}$ cm⁻³ and 2.5×10^{16} cm⁻³, respectively. The resistances of samples were ~ 140 – 400 Ω depending on their dimensions. It was supposed that, in such p -type layers, one can observe not only the room-temperature sub-THz responsivity but also the IR one.

The detected IR spectra for one of the detectors (with a design depicted in Fig. 1) are shown in Fig. 2 at $T = 78$ K and 300 K. The IR photo-response was obtained using a globar as the source of IR radiation with the temperature $T \approx 1600$ C and an IR monochromator as a spectral instrument. As a dispersive element in an SPM-2 monochromator, the

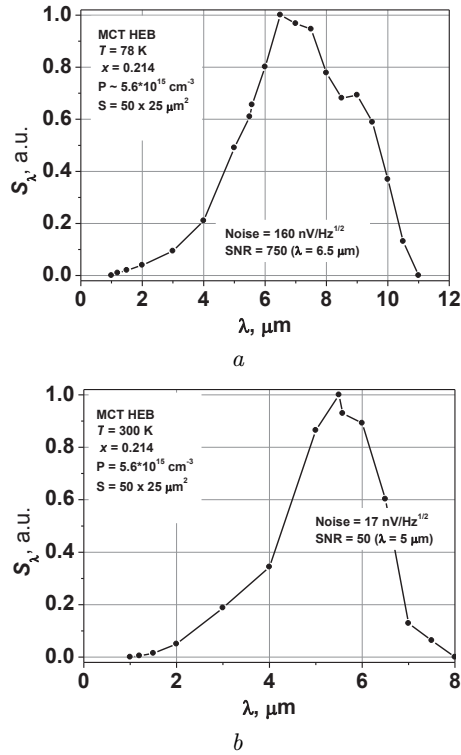


Fig. 2. Responsivity spectra S_λ of an MCT detector in the IR region *a* – $T = 78$ K, *b* – $T = 300$ K

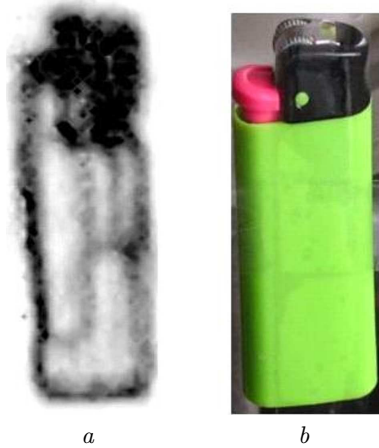


Fig. 3. *a* – the image of a lighter in a nontransparent envelope and through a 12-mm gypsum plasterboard, $\nu \approx 150$ GHz; *b* – visible image. Continuous source power $P \approx 15$ mW

NaCl prism was used with the spectral resolution $\Delta\lambda \approx 0.1 \mu\text{m}$. Detectors were current-biased with $I_{\text{bias}} = 50\text{--}100 \mu\text{A}$. The IR photoresponse (and also the sub-THz one) was measured with a lock-in amplifier (Stanford SR 830).

For the active vision in the sub-THz/THz region, the radiation frequency range $\nu \sim 150\text{--}300$ GHz can be suitable, since in this frequency range, the output power of sub-THz solid-state small size sources is easily gaining a power of 15–50 mW. As the frequency increases, the power of solid state sources is changing proportionally $\sim \nu^{-2}$, thus quickly decreasing up to $\nu \sim 1$ THz, where the so-called THz gap is situated (see, e.g., [4]). At the same time, the sensitivity of sub-THz/THz detectors is decreasing also $\sim \nu^{-2} - \nu^{-4}$, quickly going down, as the frequency increases up to the far IR spectra region.

In the sub-THz range of radiation frequency $\nu \approx 140$ GHz in MCT detectors under study, the noise equivalent power was $\text{NEP} \approx 10^{-9} \text{ W/Hz}^{1/2}$, quickly going down according to the dependence indicated above. Thus, these single uncooled direct detection detectors with a time response about the lifetime ($\tau \sim 5 \times 10^{-8}$ s) can be used only for the active imaging that was successfully demonstrated [16] in a sub-THz imaging system at the radiation frequency $\nu \approx 150$ GHz in a system with two-coordinate mechanical scanning and hyperbolic lenses, which allowed one to obtain diffraction-limited spots.

The example of a sufficient spectral resolution in the radiation frequency range $\nu \approx 150$ GHz for the lighter image with a room-temperature MCT sub-THz detector is shown in Fig. 3. The image was taken for a lighter in the envelope non-transparent for visible light and through a 12-mm gypsum plasterboard. One can clearly see the different liquid gas levels in two cells of a lighter.

3. Conclusions

It was shown that the thin MCT layers having intrinsic conductivity at room temperature can be successfully applied both to the IR and sub-THz/THz detectors, though these detectors in the latter case can be used only for the active vision.

The author thanks S. Dvoretzkii for supplying the MCT layers, V. Petriakov for the preparation of detectors, and V. Zabudsky and A. Golenkov for measuring some parameters of detectors.

1. A. Rogalski, *Infrared Detectors* (CRC Press, New York, 2011).
2. <http://solarlove.org/top-solar-module-manufacturers-2013/>.

3. S. Del Sordo, L. Abbene, E. Caroli, A.M. Mancini, A. Zappettini, and P. Ubertini, *Sensors* **9**, 3491 (2009).
4. F. Sizov and A. Rogalski, *Progr. Quant. Electr.* **34**, 278 (2010).
5. F. Sizov, V. Reva, A. Golenkov, and V. Zabudsky, *J. Infrared Milli Terahz Waves* **32**, 1192 (2011).
6. V.N. Dobrovolsky and F.F. Sizov, *Semicond. Sci. Technol.* **22**, 103 (2007).
7. V. Dobrovolski and F. Sizov, *Optoelectr. Rev.* **18**, 250 (2010).
8. F. Sizov, V. Petriakov, V. Zabudsky, D. Krasilnikov, M. Smoliy, and S. Dvoretzki, *Appl. Phys. Lett.* **101**, 082108 (2012).
9. A. Bergeron, L. Marchese, É. Savard, L. LeNoc, M. Bolduc, M. Terroux, D. Dufour, D. Tang, F. Châteauneuf, and H. Jerominek, *Proc. SPIE* **8188**, 81880I (2011).
10. A.G. Davies, A.D. Burnett, W.H. Fan, E.H. Linfield, and J.E. Cunningham, *Mater. Today*, **11**, 18 (2008).
11. *Terahertz Spectroscopy and Imaging*, edited by K.-E. Peiponen, J.A. Zeitler, and M. Kuwata-Gonokami (Springer, New York, 2013).
12. G.C. Holst, *Electrooptical Imaging System Performance* (SPIE Opt. Eng. Press, Bellingham, 1995).
13. J.L. Hesler and T.W. Crowe, *Proc. of 32nd International Conference on Infrared and Millimeter Waves, IRMMW-THz* (2007), p. 844.
14. M. Hoeffle, K. Haehnsen, I. Oprea, O. Cojocari, and R. Jakob, *J. Infrared Milli. Terahz Waves* **35**, 891 (2014).
15. G. Chekanova, M. Nikitin, I. Lartsev, V. Varavin, and N. Michailov, in: *Photoreceivers on the base of a mercury-cadmium-telluride epitaxial system*, edited by A. Aseev (SB RAS, Novosibirsk, 2012), p. 202–207.
16. F. Sizov, V. Zabudsky, A. Golenkov, and A. Shevchik-Shekera, *Optical Eng.* **52**, 033203 (2013).

Received 11.09.14

Ф. Сізюв

НЕОХОЛОДЖУВАНІ ОПТОЕЛЕКТРОННІ
ПРИЛАДИ НА ОСНОВІ НАПІВПРОВІДНИКА HgCdTe
У ШИРОКОМУ СПЕКТРАЛЬНОМУ ДІАПАЗОНІ

Резюме

В статті обговорюються результати досліджень, які пов'язані з розвитком та використанням інфрачервоних (ІЧ) та суб-терагерцових (ТГц) приймачів випромінювання, що базуються на напівпровіднику HgCdTe. Показано, що напівпровідник КРТ (кадмій–ртуть–телур) може бути застосованим для створення “двокольорового” детектора, який працює у ІЧ та суб-ТГц діапазонах спектра.